

Laser Desorption/Ionization of Transition Metal Atoms and Oxides from Solid Argon

Lester Andrews,^{*,†} Andreas Rohrbacher, Christopher M. Laperle, and Robert E. Continetti

Department of Chemistry and Biochemistry, 0314, University of California, San Diego, 9500 Gilman Drive, La Jolla, California 92093-0314

Received: March 31, 2000; In Final Form: June 26, 2000

The oxides TiO, CrO, and CoO, formed by reaction of the laser-ablated metal atoms and O₂ in excess argon during condensation at 10 K, have been laser desorbed/ionized from solid argon with 308 nm radiation for observation by TOF mass spectrometry. Mass peaks for Ti⁺, Cr⁺, Co⁺, and particularly TiO⁺ and CrO⁺ were enhanced by adding to the copper support a thin film of organic acid typically used as a matrix in matrix-assisted laser desorption/ionization (MALDI) mass spectrometry. Adding the C₆H₅Br chromophore to the Ar/O₂ gas mixture also enhanced the metal and oxide ion signals. The laser desorption/ionization (LDI) process in these cryogenic experiments with low ionization energy subject atoms and molecules is assisted by the organic acid and bromobenzene chromophores, suggesting that charge exchange plays an important role in this process.

1. Introduction

Matrix isolation spectroscopy (MIS) using inert gas hosts at cryogenic temperatures has been widely used to prepare and trap novel reactive molecular species including cations and anions for spectroscopic study.^{1–7} In particular, laser ablation has been used to provide transition metal atoms for reactions with small molecules to produce new molecular species for spectroscopic study.^{3–10} In recent years matrix-assisted laser desorption/ionization (MALDI) spectroscopy using organic acid hosts at room temperature has been employed to identify large nonvolatile bio-molecules such as peptides, proteins, and oligosaccharides,^{11–16} to monitor protein folding¹⁷ and H/D exchange in proteins,¹⁸ and for peptide mapping,¹⁹ to name a few examples. This method has been applied to frozen DNA solutions at about 180 K.²⁰ Motivated by these results, we have carried out laser desorption/ionization (LDI) experiments on cryogenic argon matrix samples at 10 K.

Mass spectrometry studies of molecules trapped in solid inert gases are relatively sparse. Michl and co-workers have employed secondary ion mass spectrometry to study rare-gas solids and to observe propane fragment ions from propane in solid argon at 10 K.²¹ Laser vaporization time-of-flight (TOF) studies have been performed on cryogenic Cl₂/Xe films.²²

New experiments performed to combine the MIS and LDI approaches for mass spectrometry on novel molecules synthesized in inert gas matrixes will be described. In the experiments reported here, laser-ablated transition metal atoms were reacted with O₂ on condensation in excess argon onto a 10 K copper plate, and metal atoms and oxides were subsequently desorbed/ionized by 308 nm radiation and accelerated into a time-of-flight mass spectrometer. The ion yields were markedly increased by precoating the copper plate with an organic acid layer or by adding bromobenzene to the gas mixture.

2. Experimental Section

Cryogenic matrix-isolation experiments were done with laser desorption/ionization of transition metal atom–dioxygen reaction products for mass spectrometric analysis. A schematic diagram of the ion source is shown in Figure 1(a) and the mass spectrometer layout is given in Figure 1(b). Typically 50 μmol of argon containing 10% O₂ was co-deposited through the spray-on line shown in Figure 1a for a 10 min period onto the LDI target, along with laser-ablated Ti, Cr, or Co atoms similar to the infrared matrix-isolation experiments.^{8–10} Based on the solid angle of the source configuration, approximately 10% of the gas sample condensed on the 10K copper plate. For ablation a focused (10 cm f.l.) doubled Nd:YLF (523.5 nm) laser with 200 μJ/pulse at 1 kHz was employed (fluence ≈ 2 J/cm²), which is expected to deposit slightly more metal atoms per unit time than the infrared experiments.^{8–10} The LDI target copper plate

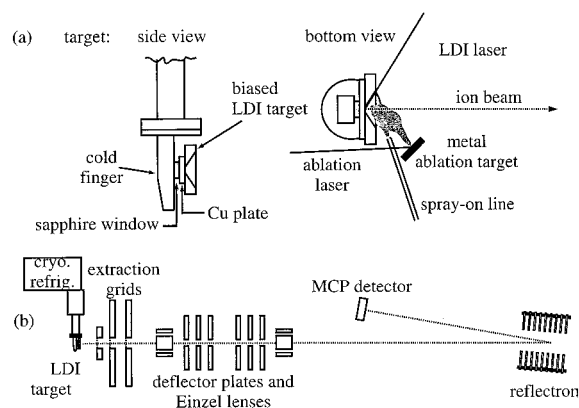


Figure 1. Schematic diagram of the cryogenic laser desorption/ionization (LDI) apparatus. (a) LDI target: the copper plate is cooled to 10 K through indium/sapphire/indium contact with a coldfinger cooled by a CTI Cryogenics Model 22 refrigerator. The metal is ablated by 523.5 nm laser radiation (200 μJ/pulse at 1 kHz, fluence ≈ 2 J/cm²) (ablation laser) and co-deposited with Ar/O₂ gas. The matrix sample is desorbed/ionized by 308 nm radiation (6–9 μJ/pulse at 20 Hz, 0.06–0.09 J/cm²) (LDI laser), (b) TOF mass spectrometer with cryogenic target.

* Author to whom correspondence should be addressed. E-mail: lsa@virginia.edu.

† Permanent address: University of Virginia, Department of Chemistry, Charlottesville, VA 22904-4319.

was attached to the cooled (CTI Cryogenics, Model 22, 10 K) oxygen-free high-conductivity copper finger through indium gasket/sapphire/indium gasket contacts, with an aluminum cover plate containing a counter-sunk 8 mm hole. The copper substrate was biased at +5.0 kV during the ablation/deposition of Ti, Cr, and Co atoms.

Time-of-flight mass spectra were recorded using focused (8 cm f.l.) XeCl excimer 308 nm radiation with 6–9 $\mu\text{J}/\text{pulse}$ at 20 Hz (fluence ≈ 0.06 – $0.09 \text{ J}/\text{cm}^2$ in a 75 ns pulse), to desorb/ionize the sample from the 10 K copper substrate biased at +5.0 kV into the apparatus shown in Figure 1b. The ions entered an electrostatic lens system consisting of two sets of deflectors and two einzel lenses. The ion beam was reflected by a commercial reflectron (R. M. Jordan) to enhance the mass resolution and detected by a microchannel plate (MCP) detector. The detected ion signal was amplified by a fast preamplifier and fed into a digital storage oscilloscope. A LabVIEW program was used to accumulate mass spectra and to record and calibrate the spectra. The pressure inside the apparatus was typically 10^{-7} Torr in the source region (pumped by a diffusion pump) and 10^{-8} Torr in the detector region (pumped by two turbo molecular pumps).

Similar experiments were done after coating the finely sanded copper plate with a film of organic acid: *trans*-3,5-dimethoxy-4-hydroxy cinnamic acid (sinapinic acid, SA), 4-hydroxy- α -cyanocinnamic acid (HCCA), or 2,5-dihydroxybenzoic acid (DHB) (Aldrich), which are used in conventional MALDI experiments.^{12,14,18,23} First, SA (saturated CH_3CN solution with 0.1% trifluoroacetic acid (TFA)) and HCCA (saturated in 50/50 $\text{CH}_3\text{CN}/\text{EtOH}$ with 0.1% TFA) were used for coating by drying 3–10 μL of solution on the copper plate at room temperature. Second, SA (saturated in 50/50 $\text{CH}_3\text{CN}/\text{H}_2\text{O}$ with no TFA) was found to give stronger ion spectra. Third, DHB (saturated in 50/50 $\text{CH}_3\text{CN}/\text{H}_2\text{O}$ and then diluted 100 times) also gave strong ion spectra.

Experiments were done with bromobenzene (Aldrich) as a chromophore both mixed at 1% with the argon and oxygen gas and as a vapor-deposited film on the copper substrate. Bromobenzene has a strong absorption from 300 to 360 nm²⁴ and is subject to two-photon ionization in the gas phase.²⁵

3. Results

Mass spectra will be presented for Ti, Cr, and Co and their monoxides formed by the reaction of laser-ablated metal atoms^{8–10} with O_2 in excess argon during condensation on a cryogenic copper substrate and on organic film coated cryogenic copper substrates.

3.1. Copper Substrate. On the copper substrate, the maximum desorption/ionization laser pulse energy, 9.1 $\mu\text{J}/\text{pulse}$ (fluence $0.09 \text{ J}/\text{cm}^2$), was required to observe ion mass spectra, and the spectra contained a number of background peaks due to traces of diffusion pump oil in the source chamber. The spectrum after reacting laser-ablated Ti with O_2 in excess argon during condensation for three 10 min periods is shown in Figure 2. Note the resolution of natural abundance Ti and TiO isotopes. The $m/z = 63$ and 65 peaks contain a minor contribution from copper. Ar^+ was observed as a weak $m/z = 40$ peak, but O_2^+ was difficult to detect.

Similar experiments were performed with Cr and Co. In each case strong atomic mass peaks were observed, again using the maximum laser energy, and background interference prevented the clear observation of CrO, but a weak CoO signal ($m/z = 75$) was observed with 5% of the intensity of Co. Weak $^{63}\text{Cu}^+$ and $^{65}\text{Cu}^+$ peaks were observed.

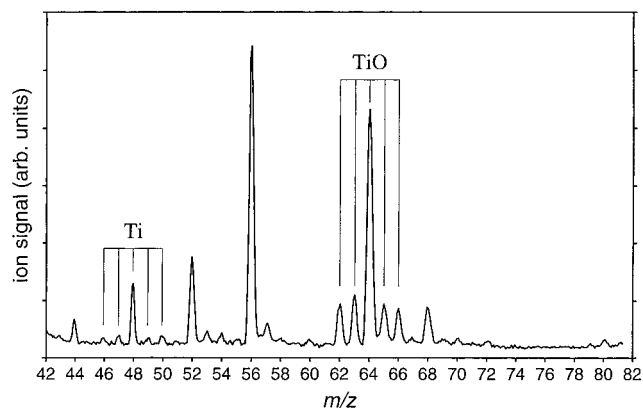


Figure 2. TOF mass spectrum obtained from $\text{Ar}/\text{O}_2 = 10/1$, sample co-deposited with laser-ablated Ti atoms for 30 min on a 10 K copper substrate. LDI at 308 nm with 9.1 $\mu\text{J}/\text{pulse}$ at 20 Hz ($0.09 \text{ J}/\text{cm}^2$).

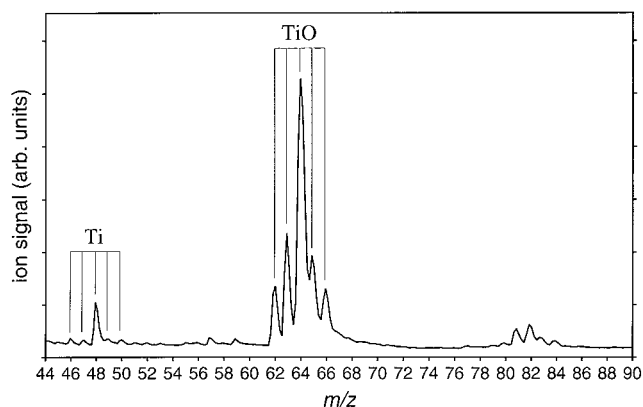


Figure 3. TOF mass spectrum obtained from $\text{Ar}/\text{O}_2 = 10/1$ sample co-deposited with laser-ablated Ti atoms for 20 min on a 10 K copper plate coated with SA (TFA) from 6 μL of dried solution. Approximately 0.10 μmol of SA on 0.5 cm^2 area. LDI at 308 nm with 6.4 $\mu\text{J}/\text{pulse}$ at 20 Hz ($0.06 \text{ J}/\text{cm}^2$).

3.2. Copper Substrate Coated with Organic Acid Film.

The same experiments were performed with organic acid coated copper substrates, and the ion signals were strong enough to reduce the desorption/ionization laser pulse energy to 6.4 $\mu\text{J}/\text{pulse}$ (fluence $0.06 \text{ J}/\text{cm}^2$). Mass spectra of the organic films contained weak $^{63}\text{Cu}^+$ and $^{65}\text{Cu}^+$ signals plus weak peaks in the background that could be due to organic fragment ions, but no organic parent ions were detected. The spectrum of Ti and O_2 from copper-supported SA film with TFA is shown in Figure 3; note the clear enhancement of the TiO signal relative to Ti and higher signal-to-noise as compared to the naked copper substrate used for the spectrum in Figure 2. The $m/z = 63$ peak contains a contribution from $^{63}\text{Cu}^+$ as well as $^{47}\text{TiO}^+$. No TiO_2 was observed, however, as the $m/z = 80$ – 84 mass peaks are due to impurities. Argon and O_2 mass peaks were barely detected above the noise level.

Figure 4 shows the spectrum for Cr and O_2 on a copper-supported-SA film (containing 130 nmol of SA). Note the strong 1/1 relative intensity CrO and Cr mass peaks with natural abundance chromium isotopes. This spectrum was reproduced in a later experiment using a fresh SA film. The initial spectrum of the copper–SA film showed weak $^{63}\text{Cu}^+$ and $^{65}\text{Cu}^+$ mass peaks, but no Cu^+ peaks were observed after the $\text{Ar}/\text{O}_2/\text{Cr}$ film was co-deposited on top of the copper–SA film. Similar experiments using SA and HCCA films containing TFA produced weaker spectra and the CrO signal was 50% and 25%, respectively, of the Cr signal. The reaction with Co on a SA

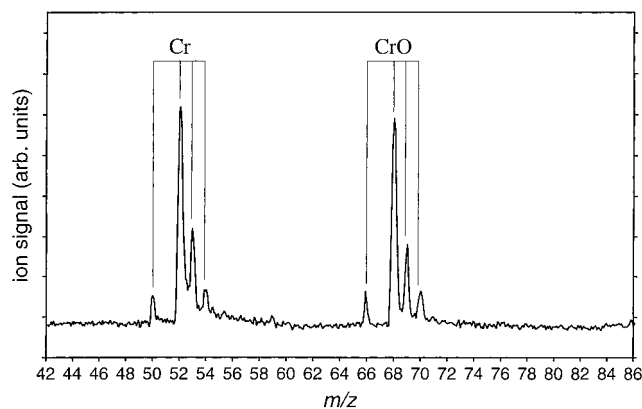


Figure 4. TOF mass spectrum obtained from Ar/O₂ = 10/1 sample co-deposited with laser-ablated Cr atoms for 20 min on a 10 K copper plate coated with SA from 6 μ L of dried saturated solution. Approximately 0.13 μ mol of SA on 0.5 cm² area. LDI at 308 nm with 6.4 μ J/pulse at 20 Hz (0.06 J/cm²).

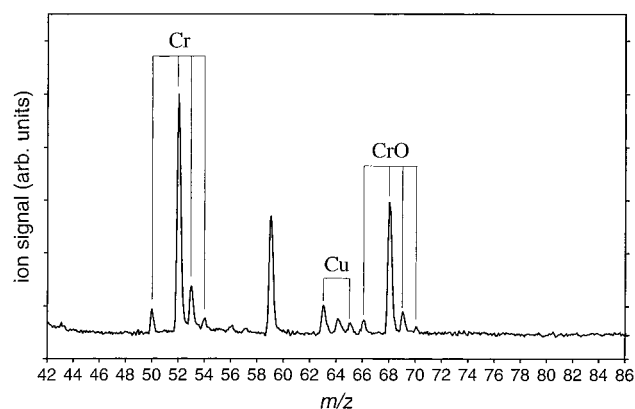


Figure 5. TOF mass spectrum obtained from Ar/O₂/C₆H₅Br = 100/10/1 sample co-deposited with laser-ablated Cr atoms for 10 min on a clean 10 K copper plate. LDI at 308 nm with 6.4 μ J/pulse at 20 Hz (0.06 J/cm²).

film produced the CoO peak at about 5% of the Co peak intensity. No metal dioxides were detected.

Experiments were done for the three metals and Ar/O₂ = 10/1 samples co-deposited onto copper-supported-DHB films (containing 100 nmol of DHB) with the same physical appearance as the above SA films. Titanium gave a spectrum of Ti⁺ and TiO⁺ similar to the SA spectrum in Figure 3. Chromium yielded a weaker Cr⁺ spectrum and a relatively much weaker CrO⁺ spectrum (CrO⁺/Cr⁺ = 1/3) than in Figure 4 using the SA film. Cobalt gave a similar Co⁺ spectrum with slightly poorer signal-to-noise, compared to SA, but no CoO⁺ was detected.

3.3. Copper Substrate plus Bromobenzene. A potential advantage of the cryogenic experiment is that volatile matrix molecules may also be used due to the low temperature of the LDI target. This was shown in experiments performed with bromobenzene as a substrate film on the 10 K copper plate and mixed at 1% with the argon/oxygen reagent gas to serve as a laser-absorbing chromophore molecule. Figure 5 shows the spectrum for a Ar/O₂/C₆H₅Br = 100/10/1 sample co-deposited with Cr for 10 min. Again the Cr⁺ and CrO⁺ signals are enhanced and the CrO⁺/Cr⁺ ratio markedly increased from spectra with Ar/O₂ samples. The $m/z = 59$ peak is variable and due to an impurity in the system. Essentially the same spectrum with half of the ion signal was observed for Cr and Ar/O₂ = 10/1 sample co-deposited on top of a C₆H₅Br film (approximately 0.04 μ mol) previously deposited by condensing

C₆H₅Br vapor from the spray-on line onto the clean 10 K copper plate.

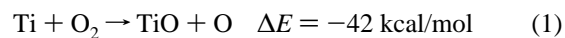
To confirm the ion-enhancing role of C₆H₅Br, a clean copper substrate was again used with Cr and only an Ar/O₂ = 10/1 cryogenic matrix; no ions were observed using a fluence of 0.06 J/cm², and only weak Cr⁺ was found with 0.09 J/cm² as reported above. Finally, another Ar/O₂/C₆H₅Br = 100/10/1 sample was co-deposited with Cr atoms, and the Figure 5 spectrum was reproduced with 0.06 J/cm². No positive ion mass peaks were observed for bromobenzene or its fragments under these argon matrix conditions; however, C⁻, C₂⁻, C₂H⁻, and C₂H₂⁻ were found in the negative ion mode.

4. Discussion

The results reported here are important for several reasons. First, these results complement cryogenic matrix infrared spectroscopy studies of transition metal–oxygen reactions.^{8–10} Second, these experiments extend the LDI process to systems synthesized in cryogenic matrixes. Finally, by studying these metal oxide systems with known ionization energies, new insights into the mechanism of the LDI process can be gained.

4.1. Cryogenic Matrix Reactions. Infrared spectra of laser-ablated transition metal atom reaction products with O₂ during condensation with excess argon at 10 K have identified the monoxide (MO) and dioxide (OMO) products.^{8–10} Identification of the MO products was based on comparison with gas-phase vibrational fundamentals and M¹⁶O/M¹⁸O isotopic frequency ratios in the matrix samples. The OMO products were also identified from oxygen isotopic shifts as well as natural abundance metal isotopes (Ti, Cr). The present mass spectra confirm the formation of metal oxides in the experiments and suggest that TiO, CrO, and CoO are reaction products. Furthermore, the observation of Ti⁺, Cr⁺, and Co⁺ mass peaks shows that not all of the ablated metal atoms react even using relatively high (10%) oxygen concentration.

The metal monoxide yields probably decrease in the order TiO > CrO > CoO as the reaction energetics require more excess energy in the metal atoms for Co > Cr to foster these endothermic reactions.²⁶ In addition, the ionization energies and therefore the difficulty for ionization increase in the series (TiO, CrO, CoO ionization energies are 6.8, 7.8, 8.9 eV, respectively).^{27–30} This explains the relative intensities of TiO⁺ > CrO⁺ > CoO⁺ mass peaks observed here.



No mass spectroscopic evidence was found for the dioxides, which have been clearly identified in the matrix infrared spectra.^{8–10} Calculated infrared intensities³¹ for TiO and TiO₂ suggest that comparable amounts of TiO and TiO₂ are produced in these experiments. The ionization energies of TiO₂ (9.5 \pm 0.5 eV)³² and CrO₂ (10.3 \pm 0.5 eV)³³ are higher, and apparently too high for the ionization method employed here. CoO₂ is expected to have an even higher ionization energy.

4.2. Laser Desorption/Ionization Processes. The observation of Ti, Cr, Co, TiO, and CrO mass spectra from solid argon matrices at 10 K is clearly enhanced by the presence of a molecule absorbing at our LDI laser wavelength (308 nm). This is shown by the *substantially reduced* desorption laser energy required to produce metal and metal oxide mass spectra and the increase in TiO/Ti and CrO/Cr mass peak intensity ratios.

CoO was observed very weakly and did not appear to be enhanced by the organic film techniques employed here. TiO₂, CrO₂, and CoO₂ were not observed in our mass spectra.

The first method employed here to assist desorption/ionization was to precipitate a layer of organic acid (SA, HCCA, or DHB) on the Cu plate at room temperature. Approximately 100–300 nmol of organic acid was applied, and the films appeared to be polycrystalline but the coverage may not be uniform. The Ar/O₂ metal atom layer was co-deposited on top of the organic layer on the copper plate cooled to 10 K. This two-layer combination markedly increased the ion yield from these samples and the intensities of TiO⁺ and CrO⁺ relative to Ti⁺ and Cr⁺ (Figures 3 and 4) as compared to identical experiments using no organic layer. Weak Cu⁺ signals were observed in some experiments (Figure 3 but not Figure 4) suggesting that the organic overlayer coverage was not uniform. Although conventional MALDI spectra usually contain peaks related to the organic matrix species,^{12,14} only weak peaks in the background could be due to organic fragment ions from the film beneath the argon matrix. We suggest that copper is much easier to detect here due to concentration of the spectrum into two ⁶³Cu⁺ and ⁶⁵Cu⁺ mass peaks instead of many fragment ion mass peaks. These fragment peaks are indistinguishable from the background pump oil signals present in the diffusion-pumped ion source. Apparently the organic chromophore cations do not survive expulsion through the argon matrix. However, with bromobenzene in the argon matrix, negative organic fragment ions were observed.

Our two-layer sample preparation is similar to the two-layer LDI experiments employing explosive compounds for enhancing the analyte mass spectra by Hakansson et al.³⁴ Both of these methods show that the absorbing substrate and the subject analyte do not have to be mixed. Since these experiments were carried out at cryogenic temperatures, we were also able to use matrix species that are volatile at room temperature, such as bromobenzene. Bromobenzene absorbs strongly at 308 nm,²⁴ and deposition of an Ar/O₂/C₆H₅Br mixture onto the cryogenic substrate with Cr atoms also worked well (Figure 5, note the weak Cu⁺ signals in Figure 5 but not Figure 4).

Given the strong enhancements observed by the addition of absorbing matrix species in these cryogenic experiments, it is of interest to consider these results in the context of the proposed mechanisms for ion formation in MALDI mass spectrometry.^{14,35–37} The most straightforward explanation for matrix cation formation is through (sequential) multiphoton ionization.^{14,35,36} It is possible that ionization of the analyte species in the experiments with only a cryogenic Ar matrix at 308 nm (4.02 eV) involves sequential multiphoton processes; we note that TiO has a 313 nm gas-phase band system²⁶ and a 308.7 nm argon matrix absorption.³⁸ The metal atom ionization energies (Ti, Cr, Co are 6.82, 6.77, 7.86 eV, respectively),³⁹ and the densities of atomic states³⁹ near 4.02 eV are also appropriate for sequential two-photon ionization processes. Strong Ti⁺, Cr⁺, and Co⁺ mass peaks were observed from the argon matrix samples. The argon matrix cannot contain metal cations from the 523.5 nm ablation process because of the +5.0 kV copper LDI substrate bias. We note that strong Ti⁺ and TiO⁺ mass peaks have been observed from vapor-deposited titanium oxide films using 265 nm excitation, which also requires two photons for ionization.⁴⁰ Similar studies done here with a precipitated chromium trioxide film and 308 nm excitation gave strong Cr⁺ and CrO⁺ signals (Cr⁺/CrO⁺ = 2/1), which again requires two-photon ionization. We conclude that multiphoton ionization of transition metal atoms and monoxides is respon-

sible for the mass peaks observed from the copper supported argon matrix samples.

Previous workers have shown that ultraviolet MALDI functions efficiently only when the laser directly excites the matrix molecules,^{12,14,41} and the results we have shown here are consistent with that. An active role for the matrix in the ionization of analyte molecules appears likely.^{12,14,42} This is further supported by our studies of known ionization energy (IE) analyte species. How are our Ti⁺, TiO⁺, Cr⁺, CrO⁺, and Co⁺ mass peaks *enhanced* by the above-described addition of organic acid or bromobenzene?

The desorption geometry clearly changes when the organic overlayer is added to the copper substrate. The greater penetration of the 308 nm laser beam into the organic layer than into copper and the resulting energy transfer to the organic layer will result in a larger volume of argon matrix expelled. However, the metal and monoxide cation yields are markedly enhanced by the added organic material. Even though the argon matrix samples contained at least 10 times more O₂ than MO (probably > 100 times), the O₂⁺ mass peak was difficult to detect. It is significant that the ionization energies of the TiO and CrO (6.8 and 7.8 eV)^{29,30} and the metal atom Ti, Cr, Co (6.82, 6.77, and 7.86 eV, respectively)³⁹ analytes are *below* the ionization energies for the organic acids (8.05 eV measured³⁶ for DHB and 8.3–8.7 eV estimated for SA from values ranging from 8.0 eV for 1,3-dimethoxybenzene, 8.4 eV for styrene, 8.5 eV for phenol, and 9.0 eV for 3-phenyl propanoic acid) and bromobenzene (9.0 eV).^{25,43} On the other hand, O₂ has a substantially higher IE (12.1 eV),⁴³ and we were not able to observe mass spectra of *i*-propanol (IE = 10.1 eV)⁴³ in a SA film experiment. This suggests that exothermic charge exchange from the organic chromophore plays an important role in assisting the ionization process for the metal atoms, TiO, and CrO investigated here. In fact, the higher IE of CoO (8.9 eV) may help explain the lower CoO⁺ ion yield in these experiments, and conversely the lower IE of TiO may justify the higher TiO⁺ ion yield. It is known that solid argon red-shifts the ionization energy of small molecules by 0.7 to 1.4 eV,⁴⁴ so even bromobenzene can be photoionized in solid argon by two 308 nm photons. Furthermore, it is also possible that two-photon excited bromobenzene energy transfers to ionize adjacent metal atoms and oxides in the matrix cage.

The involvement of charge exchange in the assisted LDI process is further supported by the observations with DHB, which has a known (8.05 eV)³⁶ and probably lower (0.3 to 0.7 eV) ionization energy than SA. We found that CrO⁺ was produced less efficiently with DHB than SA films, which we believe is a consequence of the CrO ionization energy (7.8 eV)³⁰ falling just under the value for DHB. The organic film ionization energies are not known, but they are expected to be slightly lower than the free molecule values (for example, 7.9 eV is reported for the (DHB)₂ dimer).¹⁴ In larger organic molecules, of course, other ionization mechanisms such as excited-state proton transfer can also play a role,^{14,42} but for the metal oxide systems discussed here, exothermic charge exchange appears to be very important.

5. Conclusions

Transition metal atoms and monoxides have been desorbed/ionized from 10 K argon matrix samples using 308 nm radiation. The ion yield is enhanced and the TiO⁺/Ti⁺ and CrO⁺/Cr⁺ ratios increased on the addition first of an organic acid precipitate layer to the copper substrate or the addition of a chromophore molecule (C₆H₅Br) to the gas mixture used to form the cryogenic

matrix. These experiments show that desorption/ionization processes in a cryogenic argon matrix can be enhanced by the addition of an absorbing component to the matrix and provide new insights into understanding the mechanism of the LDI process. The efficient production of TiO^+ and CrO^+ from the molecules with known ionization energies lower than the light-absorbing matrix molecules suggests that charge exchange makes an important contribution to the LDI process.

Acknowledgment. This work was supported by the Department of Energy (DOE) under Grant DE-FG03-98ER14879. The authors gratefully acknowledge the contributions of J. Kessler, R.W. Liu, and S. Dobrin in construction of the apparatus, loan of a Model 22 refrigerator from CTI Cryogenics, organic acid samples from E. A. Komives, and helpful discussions with S. Dobrin and J. Shabanowitz. L.A. is a Sesquicentennial Associate of the University of Virginia. R.E.C. is a Camille Dreyfus Teacher-Scholar, an Alfred P. Sloan Research Fellow, and a Packard Fellow in Science and Engineering.

References and Notes

- (1) Jacox, M. E. *Chem. Phys.* **1994**, *189*, 149.
- (2) Bondybey, V. E.; Smith, A. M.; Agreiter, J. *Chem. Rev.* **1996**, *96*, 2113.
- (3) Zhou, M. F.; Andrews, L. *J. Am. Chem. Soc.* **1998**, *120*, 11499 (NiCO^-).
- (4) Zhou, M. F.; Andrews, L. *J. Am. Chem. Soc.* **1998**, *120*, 13230 (OScCO^+).
- (5) Zhou, M. F.; Andrews, L. *J. Chem. Phys.* **1999**, *110*, 10370 (FeCO).
- (6) Citra, A.; Andrews, L. *J. Am. Chem. Soc.* **1999**, *121*, 11567 (NOsN).
- (7) Zhou, M. F.; Andrews, L. *J. Am. Chem. Soc.* **1999**, *121*, 9171 ($\text{RhCO}^{+, \text{a}, -}$).
- (8) Chertihin, G. V.; Andrews, L. *J. Phys. Chem.* **1995**, *99*, 6356 (TiO).
- (9) Chertihin, G. V.; Bare, W. D.; Andrews, L. *J. Chem. Phys.* **1997**, *107*, 2798; Zhou, M. F.; Andrews, L. *J. Chem. Phys.* **1999**, *111*, 4230 (CrO).
- (10) Chertihin, G. V.; Citra, A.; Andrews, L.; Bauschlicher, C. W., Jr. *J. Phys. Chem. A* **1997**, *101*, 8793 (CoO).
- (11) Beavis, R. C.; Chait, B. T. *Proc. Natl. Acad. Sci.* **1990**, *87*, 6873.
- (12) Karas, M.; Bahr, U.; Giessmann U. *Mass Spectrom. Rev.* **1991**, *10*, 335.
- (13) Hillenkamp, F.; Karas, M.; Beavis, R. C.; Chait, B. T. *Anal. Chem.* **1991**, *63*, 1193A.
- (14) Zenobi, R.; Knochenmuss, R. *Mass Spectrom. Rev.* **1998**, *17*, 337.
- (15) Burlingame, A. L.; Boyd, R. K.; Gaskill, S. J. *Anal. Chem.* **1996**, *68*, 643R. Wyttenbach, T.; Vonhelden, G.; Bowers, M. T. *J. Am. Chem. Soc.* **1996**, *118*, 8355.
- (16) Mouradian, S.; Nelson, C. M.; Smith, L. M. *J. Am. Chem. Soc.* **1996**, *118*, 8639. Gimonkinsel, M.; Prestonschaffter, L. M.; Kinsel, G. R.; Russell, D. H. *J. Am. Chem. Soc.* **1997**, *119*, 2534.
- (17) Kriwacki, R. W.; Wu, J.; Siuzdak, G.; Wright, R. E. *J. Am. Chem. Soc.* **1996**, *118*, 5320.
- (18) Mandell, J. G.; Falich, A. M.; Komives, E. A. *Proc. Natl. Acad. Sci. U.S.A.* **1998**, *95*, 14705. Mandell, J. G.; Falich, A. M.; Komives, E. A. *Anal. Chem.* **1998**, *70*, 3987.
- (19) Navale, V.; Kaushal, P.; Hunt, S.; Bunducea, I.; Gentz, R.; Kahn, F.; Vertes, A. *Anal. Biochem.* **1999**, *267*, 125.
- (20) Hunter, J. M.; Lin, H.; Becker, C. H. *Anal. Chem.* **1997**, *69*, 3608.
- (21) Orth, R. G.; Jonkman, H. T.; Powell, D. H.; Michl, J. *J. Am. Chem. Soc.* **1981**, *103*, 6026. Jonkman, H. T.; Michl, J. *J. Chem. Soc., Chem. Commun.* **1978**, 751.
- (22) Campos, F. X.; Waltman, C. J.; Leone, S. R. *Chem. Phys. Lett.* **1993**, *201*, 399.
- (23) Beavis, R. C.; Chait, B. T. *Rapid Commun. Mass Spectrom.* **1989**, *3*, 432.
- (24) NIST Chemistry Web Book (<http://webbook.nist.gov/chemistry>).
- (25) Dietz, T. G.; Duncan, M. A.; Liverman, M. G.; Smalley, R. E. *J. Chem. Phys.* **1980**, *73*, 4816.
- (26) Huber, K. P.; Herzberg, G. *Constants of Diatomic Molecules*; Van Nostrand, New York, 1979.
- (27) Dyke, J. M.; Gravenor, B. W. J.; Josland, G. D.; Lewis, R. A.; Morris, A. *Mol. Phys.* **1984**, *53*, 465.
- (28) Sappey, A. D.; Eiden, G.; Harrington, J. E.; Weisshaar, J. C. *J. Chem. Phys.* **1989**, *90*, 1415.
- (29) Dyke, J. M.; Gravenor, B. W. J.; Lewis, R. A.; Morris, A. *Faraday Trans. 2* **1983**, *79*, 2083.
- (30) Armentrout, P. B.; Halle, L. F.; Beauchamp, J. L. *J. Chem. Phys.* **1982**, *76*, 2449.
- (31) Gaussian 94, Density functional theory, BP86, 6-311+G* basis set: TiO 1015.1 cm^{-1} (167 km/mol), TiO_2 977.2 cm^{-1} (377 km/mol).
- (32) Balduchi, G.; Gigli, G.; Guido, M. *J. Chem. Phys.* **1985**, *83*, 1913 (TiO_2).
- (33) Grimley, R. T.; Burns, R. P.; Ingram, M. G. *J. Chem. Phys.* **1961**, *34*, 644 (CrO_2).
- (34) Hakansson, K.; Zubarev, R. A.; Coorey, R. V.; Talrose, V. L.; Hakansson, P. *Rapid Commun. Mass Spectrom.* **1999**, *13*, 1169.
- (35) Ehring, H.; Karas, M.; Hillenkamp, F. *Org. Mass Spectrom.* **1992**, *27*, 427.
- (36) Karbach, V.; Knochenmuss, R. *Rapid Commun. Mass Spectrom.* **1998**, *12*, 968.
- (37) Johnson, R. E. Models for Matrix-Assisted Laser Desorption and Ionization: Maldi. In *Large Ions: Their Vaporization, Detection and Structural Analysis*; Baer, T., Ng, C. Y., Powis, I., Eds.; John Wiley: New York, 1996.
- (38) Powell, D.; Brittain, R.; Vala, M. *Chem. Phys.* **1981**, *58*, 355.
- (39) Moore, C. E. *Natl. Stand. Ref. Data Ser.*, Natl. Bur. Stand. NSRDS-NBS, **1970**, 34.
- (40) Michiels, E.; Mauney, T.; Adams, F.; Gijbels, R. *Int. J. Mass Spectrom. Ion Processes* **1984**, *61*, 231.
- (41) Karas, M.; Bachmann, D.; Hillenkamp, F. *Anal. Chem.* **1985**, *57*, 2935.
- (42) Breuker, K.; Knochenmuss, R.; Zenobi, R. *J. Am. Soc. Mass Spectrom.* **1999**, *10*, 1111.
- (43) Rosenstock, H. M.; Draxl, K.; Steiner, B. W.; Herron, J. T. *J. Phys. Chem. Ref. Data* **1977**, *6*, supp. no. 1; *Handbook of Chemistry and Physics*; Lide, D. R., Ed.; CRC Press: Boca Raton, FL, 1995.
- (44) Gedanken, A.; Raz, G.; Jortner, J. *J. Chem. Phys.* **1973**, *58*, 1178.